Revista de Metalurgia
October–December 2020, 56 (4), e178
ISSN-L: 0034-8570
https://doi.org/10.3989/revmetalm.178

Synthesis and structural characterization of Fe based $Ti+Ni_3Al+Al_2O_3$ reinforcement composite produced by mechanical alloying

Tanju Teker[a,✉], S. Osman Yilmaz[b]

[a]Adıyaman University, Faculty of Engineering, Department of Metallurgical and Materials Engineering, 02040, Adıyaman, Turkey
[b]Namık Kemal University, Faculty of Engineering, Department of Mechanical Engineering, 59500, Çorlu, Tekirdağ, Turkey

(✉Corresponding author: tteker@adiyaman.edu.tr)

Submitted: 11 March 2020; Accepted: 13 October 2020; Available On-line: 22 December 2020

ABSTRACT: The Fe-based $Ti+Ni_3Al+Al_2O_3$ powder mixture is mechanically alloyed in a Spex ball mill. Composites with Fe-based $Ti+Ni_3Al+Al_2O_3$ addition were produced at 1000 °C sintering temperature for 1 h sintering time. The metallurgical properties of these composites were examined by scanning electron microscopy (SEM), optical microscopy (OM), energy dispersive spectroscopy (EDS), X-ray diffraction (XRD) and microhardness analyses. The final products produced by mechanical alloying were nanocrystalline nickel-rich solid solution and the size of average crystallite was in the range of a few nanometres. Titanium content in the reinforcement increased microhardness values of composite. The produced composites included Fe_3Al, TiAl, NiAl, Al_3Ni_2, Al_2O_3 and Fe_3O phases.

KEYWORDS: Al_2O_3; Ball milling; Microhardness; Ni_3Al; Sintering

Citation/Citar como: Teker, T.; Yilmaz, S.O. (2020). "Synthesis and structural characterization of Fe based $Ti+Ni_3Al+Al_2O_3$ reinforcement composite produced by mechanical alloying". *Rev. Metal.* 56(4): e178. https://doi.org/10.3989/revmetalm.178

RESUMEN: *Síntesis y caracterización estructural del compuesto de refuerzo de $Ti+Ni_3Al+Al_2O_3$ a base de Fe producido por aleación mecánica*. La mezcla de polvo de $Ti+Ni_3Al+Al_2O_3$ a base de Fe se alea mecánicamente en un molino de bolas Spex. Los compuestos con adición de $Ti+Ni_3Al+Al_2O_3$ a base de Fe se produjeron a una temperatura de sinterización de 1000 °C durante un tiempo de 1 h. Las propiedades de estos compuestos se examinaron mediante microscopía electrónica de barrido (SEM), microscopía óptica (OM), espectroscopía de dispersión de energía (EDS), difracción de rayos X (XRD) y análisis de microdureza. El producto final producido por aleación mecánica fue una solución sólida rica en níquel nanocristalina, el tamaño promedio del cristal era de unos pocos nanómetros. El contenido de titanio en el refuerzo aumentó los valores de microdureza del composite. Los compuestos producidos incluían las fases Fe_3Al, TiAl, NiAl, Al_3Ni_2, Al_2O_3 y Fe_3O.

PALABRAS CLAVE: Al_2O_3; Molino de bolas; Microdureza; Ni_3Al; Sinterización

ORCID ID: Tanju Teker (https://orcid.org/0000-0001-7293-0723); S. Osman Yilmaz (https://orcid.org/0000-0001-7593-6135)

1. INTRODUCTION

The complex shaped parts can be manufactured easily at the desired sizes by powder metallurgy (P/M) method. Innovations in powder metallurgy facilitate to the production of complex machine parts of high quality and with low tolerances. In order to contribute to the mechanical properties of the parts produced by P/M method, various alloying elements or particles can be used as reinforcing components into the metal matrix and new materials can be produced in different properties and desired shapes (Hwang *et al*., 1992; Coreño Alonso *et al*., 2000; Suryanarayana, 2001; Sheng *et al*., 2010). The selection of the appropriate matrix and reinforcing element is crucial in order to obtain excellent physical and mechanical properties in composites. The interaction between the matrix and reinforcing element should therefore be strong. The main function of the reinforcing element in composite materials is to carry the loads and thus ensure that the matrix is rigid and durable. Generally, desired properties of materials are high strength, low density, having a mixture of covalent-ionic bonds. One of the limits of modern technology is difficult to obtain metal alloys having different melting point. For example, metals with low melting point cannot be alloyed with metals with high melting point by conventional methods (Enayati *et al*., 2004; Moshksar and Mirzaee, 2004; Wieczorek-Ciurowa and Gamrat, 2005; Zelaya *et al*., 2013; Chérif *et al*., 2016).

However, in recent years, conventional alloying methods have been replaced by "mechanical alloying" (MA). With the MA method, productions of metal and metal oxides are recognised effectively. In the MA method, it is ensured that composites having homogeneous microstructure are produced by providing the powders to be welded continuously to each other and then fracturing these welds. The powders in the closed container are alloyed by rotating with the help of a shaft. Powders are broken with the help of balls and cold boiling occurs. It is difficult for the metals and oxides to form phases with each other by classical methods (Eckert *et al*., 1992; Krivoroutchko *et al*., 2000; Pippan *et al*., 2006; Sheu *et al*., 2009; Liu *et al*., 2014). Forouzanmehr *et al*. (2009), examined the synthesis and description of γ-TiAl-αAl_2O_3 nanocomposite with MA. After grinding, the fcc-TiAl/α-Al_20_3 powder alloy was achieved. Throughout annealing, steady fcc-TiAl was changed into γ-TiAl.

In this study, Fe-based Ti+Ni_3Al+Al_2O_3 powder compound is mechanically alloyed in a spex ball mill. The composites with Fe-based Ti+Ni_3Al+Al_2O_3 addition were produced at 1000 °C sintering temperature for 1 h sintering time.

2. EXPERIMENTAL PROCEDURES

Fe powder (150 μm) as matrix and Ti+Ni_3Al+Al_2O_3 powder (100–150 μm) as reinforcement were used. The chemical compositions of the powders used in produced samples were given in Table 1. Ti, Ni_3Al and Al_2O_3 powders were subjected to mechanical alloying at the rate of 50% + 25% + 25%. Spex type (1200 rev·min^{-1}) high energy grinding mill was used in mechanical alloying. Ball diameter, ball/powder ratio, mechanical alloying time were selected as 10 mm, 1/10 and 15 min, respectively. Ti+Ni_3Al+Al_2O_3 reinforcements obtained from the mechanical alloying process. Ti+Ni_3Al+Al_2O_3 powders were added to the Fe matrix in different ratio of 0.5, 1, 3, 5, 7, 12 and 15 wt.%. The powders were located in the cold press die and pressure of 25 MPa was applied. The samples were sintered at 1000 °C. The production parameters of experimental samples were represented in Table 2.

Samples for microstructural evaluation were prepared by grinding, polishing and then the samples etched with nitric acid. The structural characterizations of the etched samples were characterized by using optical microscope (OM; Leica DM750), scanning electron microscopy (SEM; Zeiss EVO LS10), energy dispersive spectroscopy (EDS) analysis. The phase and compound characterization of the microstructure were detected by X-ray diffraction device (XRD; Bruker) using (λ= 1.5418 Å) CuKα radiation. Microhardness values were determined on microhardness tester (Qness Q10) at load of 25 g for 10 s.

3. RESULTS DISCUSSION

3.1. Evaluation of microstructural properties

In Fig. 1, SEM micrographs of the 0.5, 3, 7 and 15 wt.% reinforced samples were given after sintering. It was seen that the sintering temperature had crucial effect on the reinforcement and diffusion. The size of grain boundaries in the structure decreased with the increase in temperature. The exothermic reaction between Fe and Ti+Ni_3Al powders during sintering created high temperature. This heat provided denser structure. Type and amount of phases were related to MA time, reinforcement rate, sintering temperature and time. Coexistence of

TABLE 1. Chemical composition of powder mixtures used in the study (wt.%)

Powder	Fe	Ti	Ni	Al	Al_2O_3	Other
Fe	99.98	-	-	-	-	0.02
Ti	-	99.95	-	-	-	0.05
NiAl	-	-	84	15.7	-	0.3
Al_2O_3	-	-	-	-	99.97	0.03

TABLE 2. Produced samples and applied test parameters

Sample N°	Fe (%)	Ti+Ni_3Al+Al_2O_3 (%)	Cu (%)	Press (Bar)	Temperature (°C)	Time (h)
S1	98.5	0.5	1	150	1000	1
S2	98	1	1	150	1000	1
S3	96	3	1	150	1000	1
S4	94	5	1	150	1000	1
S5	92	7	1	150	1000	1
S6	87	12	1	150	1000	1
S7	84	15	1	150	1000	1

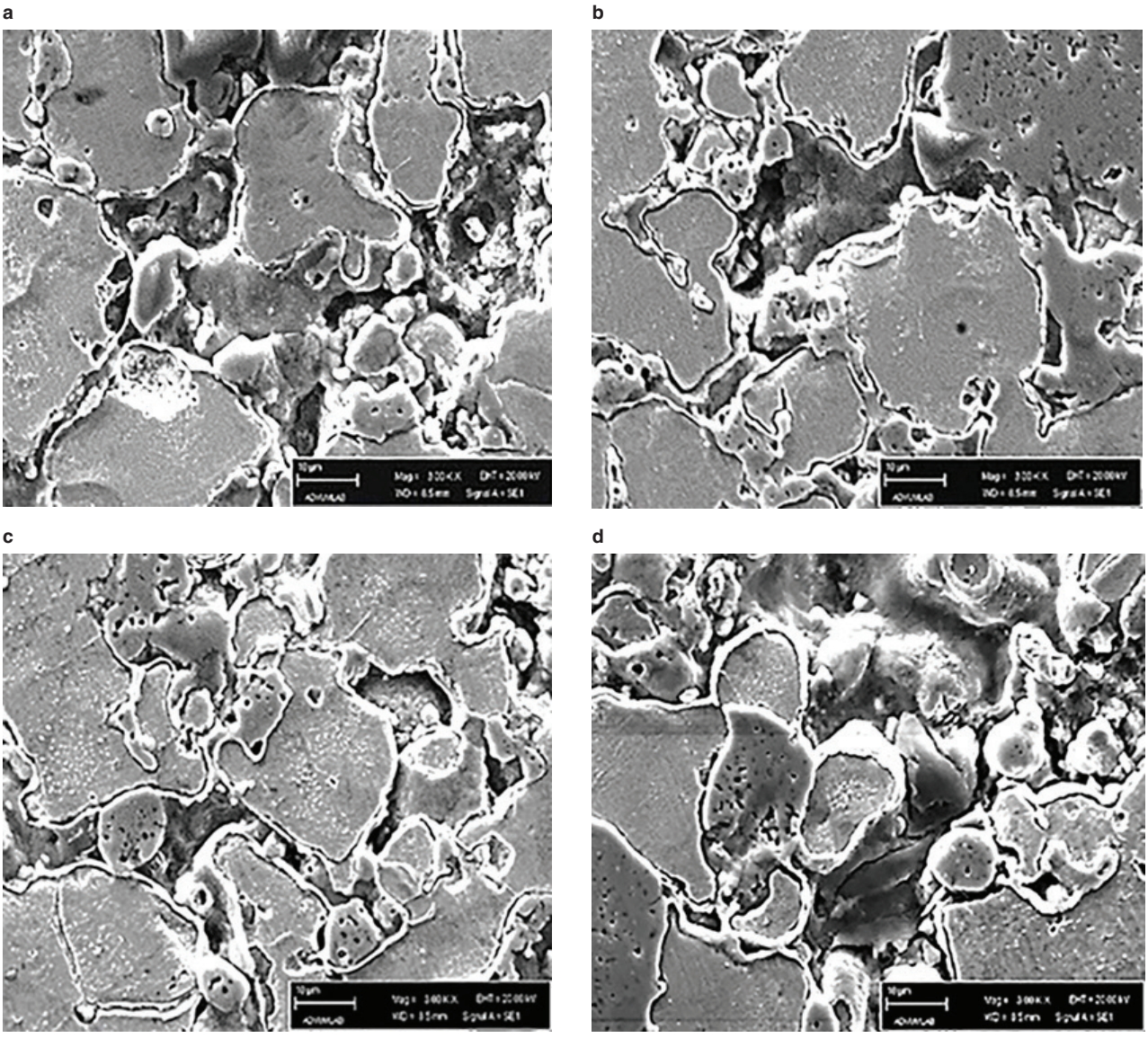

FIGURE 1. SEM micrographs of a) S1, b) S3, c) S5 and d) S7 samples.

great and minor particles in the microstructure may be associated with the propensity of lesser particles to weld together and the tendency of great particles to break under stable-state terms (Krivoroutchko *et al*., 2000; Pippan *et al*., 2006). The final products were remarkably influenced by the addition of Ti. The morphology of Ni-Al-Ti powders were quite dissimilar from each other and the particle size was very bigger than the (fcc) Ni-Al solid solution formed. Also, Ni-Al-Ti powders revealed excessively plastic distortion during MA. Therefore, cold welding facilitated powder breaking during mechanical milling and caused lower powder particles. In addition, the fragility of the powders increased during the long grinding time, which resulted in the formation of smaller particles having hemispherical shape. The presence of various crystal defects in the structure increased the dispersion of dissolved elements into matrix. After sintering, $NiAl_3$ compound was formed in the microstructure. This compound then reacted with Fe in order to form FeNiAl. Ni_3Al was dissolved in the matrix depending on the presence of Fe. Consequently, during sintering, FeNiAl and Ni_3Al intermetallic phases were formed. It was seen that the Al_2O_3 particles were partially dissolved and their size decreased.

Depending on the Ti density, the dissolution temperature of the Al_3Ni phase increased and the Al_3Ni_2 phase was not seen in the structure. $Ti+Ni_3Al+Al_2O_3$ reinforcement particles increased the Ni_3Al volume fraction. The intergranular phase was NiAl, the matrix was Ni_3Al. The size of the secondary phase between the grain boundaries increased, and the size of the grains also decreased with the sintering temperature. The melting of Al-rich phase facilitated the sintering process, and the sintering reaction involved the reactions of a certain interaction between solid Ni and Al-rich liquid phase. Depending on the sintering temperature, more or less NiAl and Ni_3Al phases could also form. The change in sintering temperature affected the liquid phase formation and the average concentration.

Ni_3Al reinforcement particles were dissolved in the structure by exothermic reactions. This solution was MA. The temperature of the exothermic reaction reached the dissolution temperature of the Ni_3Al reinforcing particles. The size of the secondary phases and pores increased in the grain boundary and the grain size decreased due to the increase in sintering temperature. The increase of Ni_3Al reinforcement changed the dissolution rate and reaction temperature. If the sintering temperature reaches the melting temperature of aluminates, impurity or pores will occur in the structure (Li *et al*., 2004). As a result, large pores occurred in some regions of matrix. In sample S7, different microstructure from matrix was formed as a result of melting of the aluminium-rich phase during sintering at 1000 °C.

The sintering reaction involved the interaction of liquid rich in solid Ni and Al. This type of interaction was often explained by reaction diffusion model. The growth in the product layer depended on atomic transfer and the growth was not related to the dissolution of the layer. The dissolution of Ni in unsaturated Al liquid can be shown. Ni_3Al phase occurs above 800 °C. The first layer was formed as a result of the solid-liquid interaction containing Al_3Ni. At the same time, the temperature increased constantly and caused the layer to gradually dissolve. When the temperature was about 800 °C, Al_3Ni started to melt in the structure. The Al_3Ni layer, which was in contact with the Ni particles, led to the formation of phases richer in Ni. The microstructure was formed by reaction mechanism that had an effect on mechanically alloyed Ni-Al powders. Looking at SEM microstructures and XRD results, Ni_3Al dissolution could be seen. Depending on the production parameters in the samples, the decrease of temperature in the reaction zone caused the reaction not being completed. Ni_3Al was dissolved at the centre of the carbide and at 800 °C, it can be seen in all carbides. The diffusion ratio of Ti atoms to Ni_3Al matrix was higher than the Ni and Al atoms diffusion ratio. As a result of the kirkendal effect, Ni_3Al dissolved and pores occurred. Looking at the XRD results, the undissolved Ni_3Al rate decreased in the S7 sample and the NiAl intermetallic rate increased.

According to the EDS analysis in Fig. 2, it was seen that the atoms of Al, Ni and Ti dissolved in the matrix. Moreover, the dissolution of these atoms changed the microstructure, and the increase in the Al_2O_3 ratio affected the Ni_3Al phase volume fraction in the microstructure. Dissolution of Al_2O_3 oxide was effective on microstructural changes because the presence of Al, Fe and Ni atoms reduced the chemical potential of Ni_3Al and the temperature of the NiAl formation system (Mao *et al*., 2003; Song *et al*., 2011). Stoichiometric Ni-Al composition was formed when liquid phase reached 50% volume fraction and the sintering temperature was between 600–700 °C, so the sintering temperature gradually increased from 600 °C to 1000 °C. When the microstructure photographs of S4 and S5 samples were compared to each other, it was observed that the size of the secondary phases of S5 sample increased in the grain borders.

As seen from SEM micrograph; Ni_3Al, Al_2O_3 and intermetallic compounds were homogeneously dispersed into particles as a result of mechanical grinding in the microstructure. The presence of Ni_3Al and Ti changed the shape of intermetallics and as seen from XRD diagrams; use of Al_2O_3 as a reinforcement particle prevented intermetallic phase formation. The reinforcement particles made of NiAlFe, Ni_3Al, TiAl, Al_3Ni_2 and Al_2O_3 phases and the matrix contained the α-Fe phase. It was concluded that the increase in

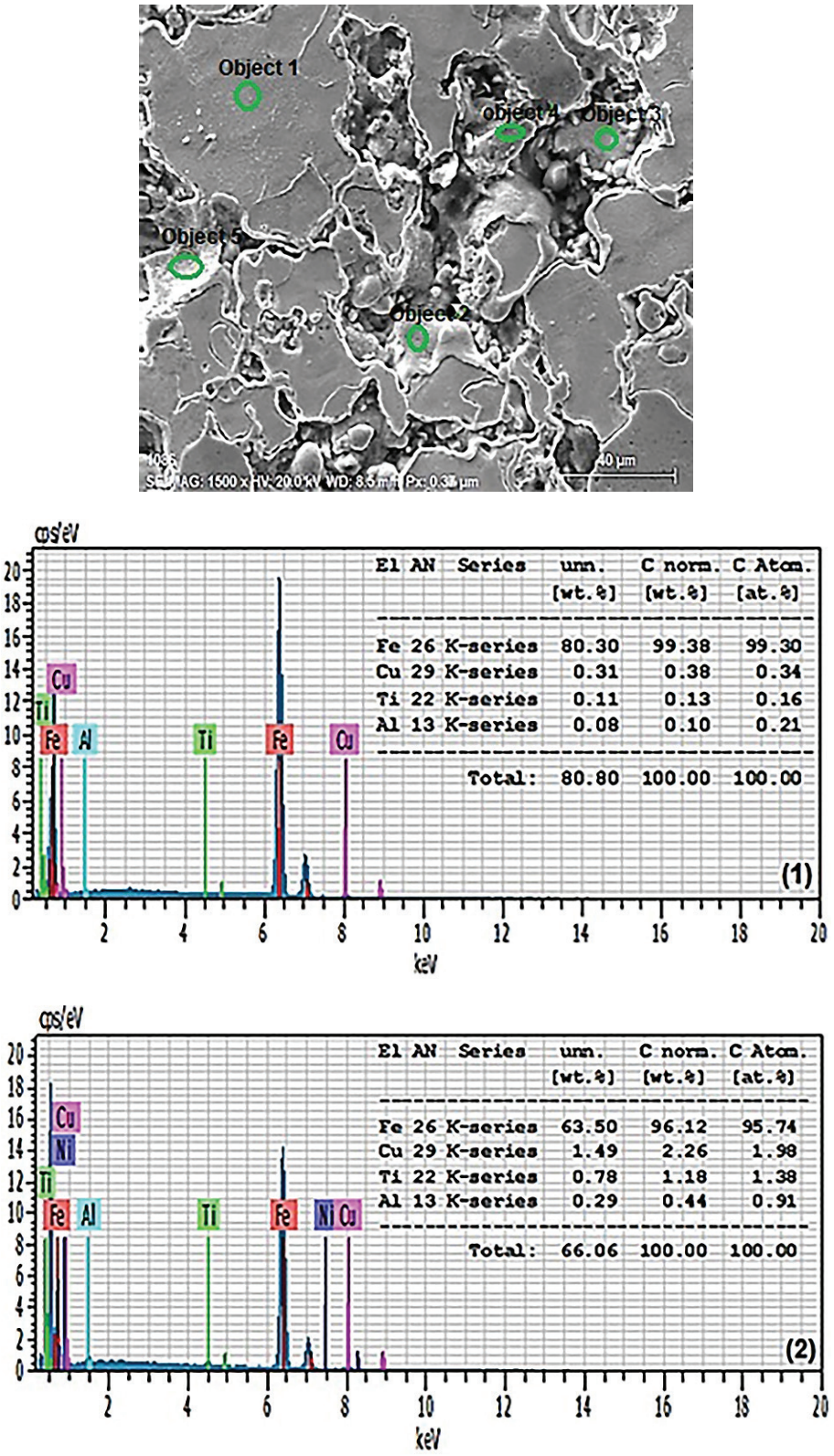

FIGURE 2. EDX analysis results of S5 sample.

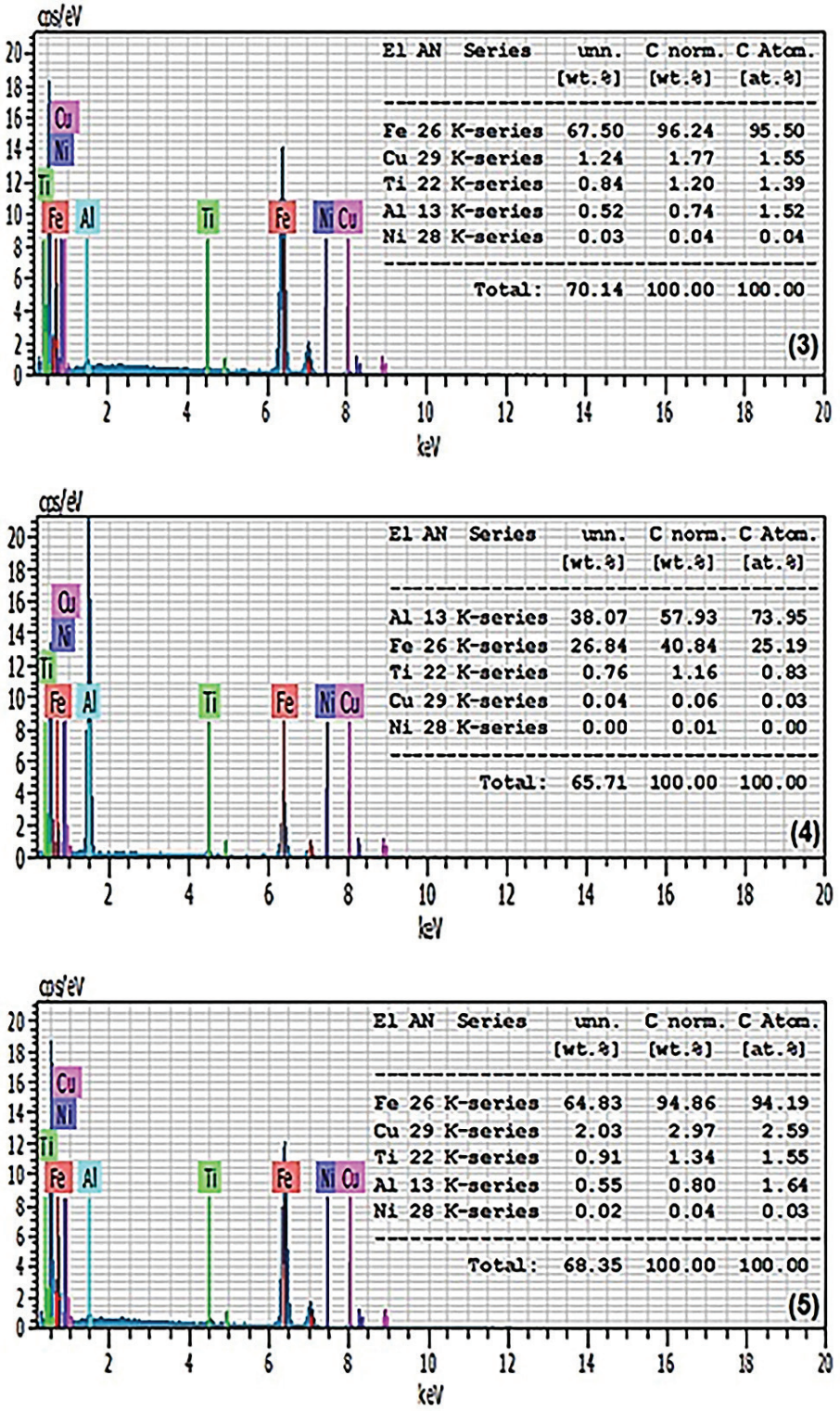

FIGURE 2. (Continued) EDX analysis results of S5 sample.

the amount of Al_2O_3 suppressed the formation of intermetallic. The increase in sintering temperature decreased Ni_3Al density, above 1000 °C, undesirable Al4N3, Al_3Ni_2 phases occurred. When the amount of reinforcement was increased, FeNiAl formation was not observed in the structure until the amount of

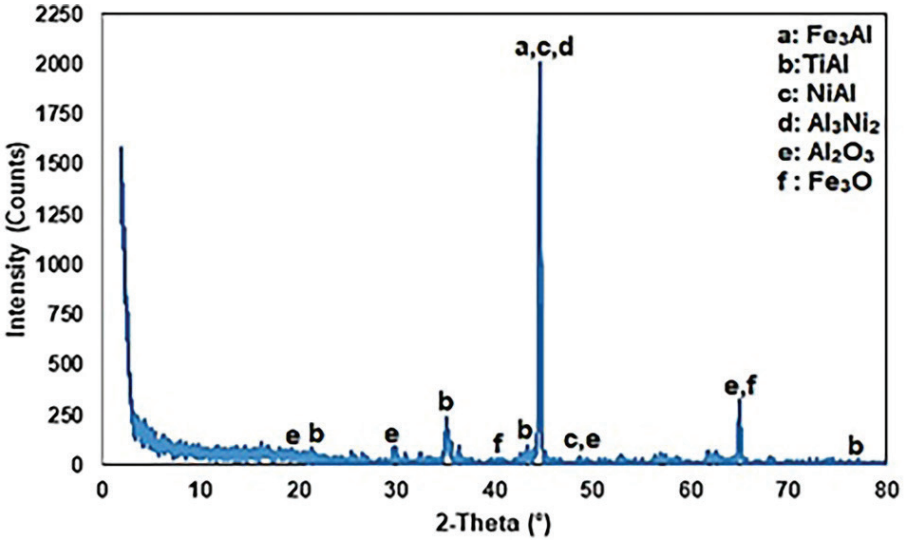

FIGURE 3. XRD graph of S3 sample.

reinforcement was 5%. FeNiAl started to form in the structure since more Ni dissolved within the matrix. As seen from SEM micrographs, the samples especially contained Fe, Ni_3Al, NiAl, Al_2O_3 and other secondary phases. The NiAl phase volume fraction was reached level of 80–85%.

The increase in the rate of reinforcement decreased the grain size and also increased the intermetallic phase and carbide ratio. The etching solution interacted with Ni_3Al faster than NiAl. White phases or precipitate phases were NiAl, grey phase or matrix was Ni_3Al. From microstructure micrograph of samples; it was seen that the Ni_3Al particles were partially dissolved in the matrix and the amount of this decreased. Depending on the formation temperature and enthalpy of the intermetallic phases, Ni_3Al had significant effect on the matrix grain size.

Al and Ti dissolution having bigger atom radius in nickel caused solid solution hardening. This situation supported the powder fragmentation throughout M.A. As can be seen in Fig. 1, the size of crystallite declined throughout the early milling time process. Subsequently, it decelerated and got progressively smaller in order to obtain a few nanometres values. The supersaturated solid solution Ni(Al,Ti) was occurred with Al and/or Ti dissolution in Ni lattice, which could be understood from Ni lattice parameter time dependency. Ni (Al, Ti) solid solution lattice parameter enhanced with the time of milling by indicating that the Ni lattice enlarged since the larger Al and Ti atoms were diffused into the Ni matrix.

3.2. XRD analysis

XRD results of S2 and S7 samples were given in Fig. 3 and Fig. 4. The produced composites included Fe_3Al, TiAl, NiAl, Al_3Ni_2, Al_2O_3 and Fe_3O phases. Regardless of composition and heat synthesis, samples had similar microstructures. As a result of the increase in sintering temperature from 650 °C to 850 °C, a smoother and gapless transition was observed between the matrix and Al_2O_3. This positive development affected microhardness values positively and values increased. At 1000 °C, where the temperature was increased even more, it was observed that the matrix phase caused the grains to grow and the hardness values decreased.

In cases where the composites were below the high sintering temperature, NiAl volume fraction increased up to 38%. After sintering, temperature reached a higher temperature than the melting temperature of all intermetallic in the Ni-Al system. This resulted in the creation and condensation of the liquid phase. The period needed to complete condensation depended on the liquid phase volume fraction in the structure. This period increased with the reduce of the liquid phase volume fraction. Ni or Al peaks was not seen in the XRD results. However, the NiAl concentration changed when the samples were compared to each other. The formation of the liquid phase in the samples increased the reaction between Al_2O_3 and other components of the composites. The long-term milling process led to the main diffraction peaks to change to small angles for mixtures of powder (Figs. 3 and 4). This change was most remarkable in the Ni-Al-Ti powder composite. In milling process, the firstly intense peaks were enlarged and decreased, which may be contributed the crystals refinement and increment of lattice strain induced throughout the MA process. Relationship between Ni-Al-Ti and Ni-Al systems was related to the influence of Ti additive in Ni-Al alloy. The reduction in the sizes of crystallite was quite marked for cubic NiAl

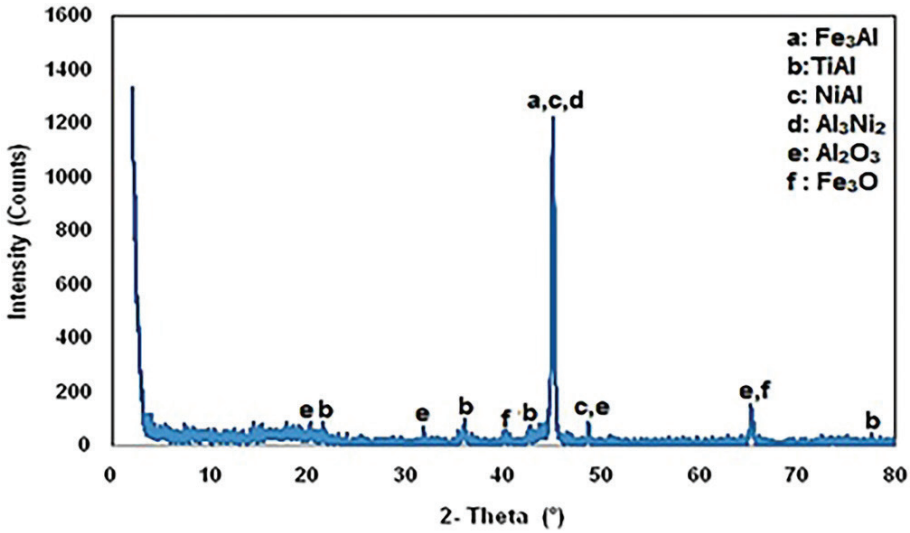

FIGURE 4. XRD graph of S7 sample.

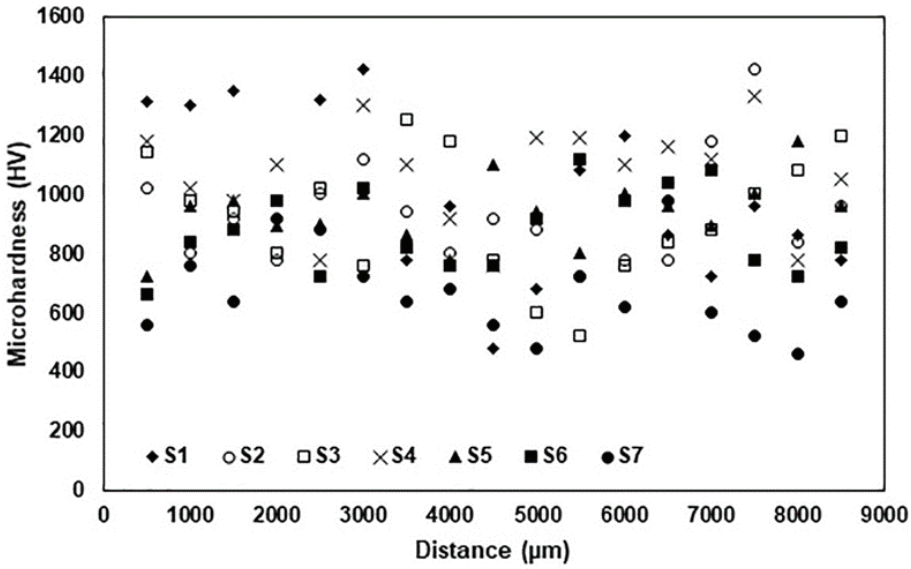

FIGURE 5. Variation of microhardness values of S1-S7 samples.

phase structure because the addition of Ti offered high ductility to NiAl phase.

3.3. Microhardness

Changes of microhardness values according to experiment parameters were given in Fig. 5. Ti, Ni_3Al, Al_2O_3 and Fe powders were mixed. Al solid solution was formed in the matrix (FeNi) of the composite. Ni_3Al and Al_2O_3 were observed in some regions and the hardness of these regions was determined as 600–1420 HV. The reason for the microhardness difference was probably due to high internal tension. The increase in the sintering temperature or the reduce in the quantity of the matrix NiAl phase in the structure did not cause a significant change in the pore volume fraction in the samples. Formation mechanism of Al_2O_3 and Ni_3Al composites could be different than the formation mechanism in pure Ni_3Al composites. Small amount of undissolved Ni_3Al particles remained in Al_2O_3-Ni_3Al composites. The formation reactions of the intermetallic phases started in the structure with the enhancement of the sintering temperature and also the creation of the liquid phase occurred (Akhtar, 2009). With the advance of the reaction, the amount of liquid phase decreased. The liquid phase disappeared upon completion of the exothermic reaction. Also, the existence of the liquid phase for a short time benefited the concentration of particles in

the secondary regions. In Al_2O_3-Ni_3Al composites, heat production and liquid phase amount resulting from exothermic reaction was less compared to pure Ni_3Al. As a result, the time needed for condensation was greater. When the amount of the matrix phase was poor, the rate of the liquid phase was not adequate to fill all the holes. Considering the change in the amount of reinforcement in the samples, it was found that the added hardness amount was 3, 5, 7 and 12 wt.%, while the microhardness values were high. However, this increase in microhardness values was not seen in the amount of 15 wt.% reinforcement.

4. CONCLUSIONS

Following findings were obtained:

- The final products contained nanocrystalline fcc-Ni(Al) and fcc-Ni(Al,Ti) solid solutions.
- The presence of Ni_3Al and Ti changed the shape of intermetallic compounds.
- The increase in the amount of Al_2O_3 suppressed intermetallic formation.
- The grain size of the composite decreased up to 1000 °C depending on the sintering temperature.
- Ideal Ti+Ni_3Al+Al_2O_3 reinforcement rate was determined as 7 wt.%.
- The resolution of Al and Ti with bigger atom radius in Ni led to solid solution hardening.
- Ti+Ni_3Al+Al_2O_3 reinforcement changed dissolution rate and effective reaction temperature.
- The dissolution of NiAlFe, Ni_3Al, TiAl, Al_4Ni_3, Al_3Ni_2 and Al_2O_3 atoms during sintering changed the microstructure.
- The increase in temperature caused to grow in the grains of the matrix phase and the hardness values decreased.
- The XRD results indicated that changes of phase occurred with increasing the amount of reinforcement.

ACKNOWLEDGMENTS

This work was financially supported by the KAYALAR copper group. The authors are grateful to KAYALAR copper Industry and Trade Incorporated Company for their financial assistance in conducting the experiments.

REFERENCES

Akhtar, F. (2009). Synthesis, microstructure and mechanical properties of Al_2O_3 reinforced Ni_3Al matrix composite. *Mater. Sci. Eng*. A. 499 (1–2), 415–420. https://doi.org/10.1016/j.msea.2008.09.005.

Chérif, A., Rekik, H., Escoda, L., Sunol, J.J., Saurina, J., Khitouni, M., Makhlouf, T. (2016). Structural and thermal characterizations of the solid-state reaction between Ni, Al, and Ti powders during mechanical alloying. *J. Therm. Anal. Calorim*. 125 (2), 721–725. https://doi.org/10.1007/s10973-016-5355-4.

Coreño Alonso, O., Cabañas-Moreno, J.G., Cruz-Rivera, J.J., Calderón, H.A., Umemoto, M., Tsuchiya, K., Quintana-Molina, S., Falcony, C. (2000). Characterization of NiAl intermetallic produced by mechanical alloying and consolidated by spark plasma sintering. *Mater. Sci. Forum* 343–346, 635–640. https://doi.org/10.4028/www.scientific.net/MSF.343-346.635.

Eckert, J., Holzer, J.C., Krill, C.E., Johnson, W.L. (1992). Investigation of nanometer-sized FCC metals prepared by ball milling. *Mater Sci. Forum* 88–90, 505–512. https://doi.org/10.4028/www.scientific.net/MSF.88-90.505.

Enayati, M.H., Sadeghian, Z., Salehi, M., Saidi, A. (2004). The effect of milling parameters on the synthesis of Ni_3Al intermetallic compound by mechanical alloying. *Mater. Sci. Eng. A*. 375–377, 809–811. https://doi.org/10.1016/j.msea.2003.10.060.

Forouzanmehr, N., Karimzadeh, F., Enayati, M.H. (2009). Synthesis and characterization of TiAl/α-Al_2O_3 nanocomposite by mechanical alloying. *J. Alloys Compd*. 478 (1–2), 257–259. https://doi.org/10.1016/j.jallcom.2008.12.047.

Hwang, S.J., Nash, P., Dollar, M., Dymek, S. (1992). The production of intermetallics based on NiAl by mechanical alloying. *Mater. Sci. Forum*. 88–90, 611–618. https://doi.org/10.4028/www.scientific.net/MSF.88-90.611.

Krivoroutchko, K., Kulik, T., Matyja, H., Portnoy, V.K., Fadeeva, V.I. (2000). Solid state reactions in Ni–Al–Ti–C system by mechanical alloying. *J. Alloys Compd*. 308 (1–2), 230–236. https://doi.org/10.1016/S0925-8388(00)00802-1.

Li, J.L., Li, F., Hu, K. (2004). Preparation of Ni/Al_2O_3 nanocomposite powder by high-energy ball milling and subsequent heat treatment. *J. Mater. Process. Tech*. 147 (2), 236–240. https://doi.org/10.1016/j.jmatprotec.2003.12.022.

Liu, E., Jia, J., Bai, Y., Wang, W., Gao, Y. (2014). Study on preparation and mechanical property of nanocrystalline NiAl intermetallic. *Mater. Des*. 53, 596–601. https://doi.org/10.1016/j.matdes.2013.07.052.

Mao, S.X., McMinn, N.A., Wu, N.Q. (2003). Processing and mechanical behaviour of TiAl/NiAl intermetallic composites produced by cryogenic mechanical alloying. *Mater. Sci. Eng. A*. 363 (1–2), 275–289. https://doi.org/10.1016/S0921-5093(03)00652-X.

Moshksar, M.M., Mirzaee, M. (2004). Formation of NiAl intermetallic by gradual and explosive exothermic reaction mechanism during ball milling. *Intermetallics* 12 (12), 1361–1366. https://doi.org/10.1016/j.intermet.2004.03.018.

Pippan, R., Wetscher, F., Hafok, M., Vorhauer, A., Sabirov, I. (2006). The limits of refinement by severe plastic deformation. *Adv. Eng. Mater*. 8 (11), 1046–1056. https://doi.org/10.1002/adem.200600133.

Sheu, H.H., Hsiung, L.C., Sheu, J.R. (2009). Synthesis of multiphase intermetallic compounds by mechanical alloying in Ni–Al–Ti system. *J. Alloys Compd*. 469 (1–2), 483–487. https://doi.org/10.1016/j.jallcom.2008.02.019.

Sheng, L., Zhang, W., Guo, J., Yang, F., Liang, Y., Ye, H. (2010). Effect of au addition on the microstructure and mechanical properties of NiAl intermetallic compound. *Intermetallics* 18 (4), 740–744. https://doi.org/10.1016/j.intermet.2009.10.015.

Song, J., Hu, W., Gottstein, G. (2011). Long term stability and mechanical properties of Al_2O_3–NiAl composites reinforced with partially fragmented long fibers. *Mater. Sci. Eng. A*. 528 (25–26), 7790–7800. https://doi.org/10.1016/j.msea.2011.07.002.

Suryanarayana, C. (2001). Mechanical alloying and milling. *Prog. Mater. Sci*. 46 (1–2), 1–184. https://doi.org/10.1016/S0079-6425(99)00010-9.

Wieczorek-Ciurowa, K., Gamrat, K. (2005). NiAl/Ni_3Al–Al_2O_3 composite formation by reactive ball milling. *J. Therm. Anal. Calorim*. 82, 719–724. https://doi.org/10.1007/s10973-005-0955-4.

Zelaya, E., Esquivel, M.R., Schryvers, D. (2013). Evolution of the phase stability of Ni–Al under low energy ball milling. *Adv. Powder Technol*. 24 (6), 1063–1069. https://doi.org/10.1016/j.apt.2013.03.008.